

Multitasking associative networks

Elena Agliari ^{*}, Adriano Barra [†], Andrea Galluzzi [‡],
Francesco Guerra [§], Francesco Moauro [¶]

12 Nov 2011

Abstract

We introduce a bipartite, diluted and frustrated, network as a sparse restricted Boltzman machine and we show its thermodynamical equivalence to an associative working memory able to retrieve multiple patterns in parallel without falling into spurious states typical of classical neural networks. We focus on systems processing in parallel a finite (up to logarithmic growth in the volume) amount of patterns, mirroring the low-level storage of standard Amit-Gutfreund-Sompolinsky theory. Results obtained through statistical mechanics, signal-to-noise technique and Monte Carlo simulations are overall in perfect agreement and carry interesting biological insights. Indeed, these associative networks pave new perspectives in the understanding of multitasking features expressed by complex systems, e.g. neural and immune networks.

1 Sparse restricted Boltzman machines as associative networks

Neural networks rapidly became the "harmonic oscillators" of parallel processing: Neurons (spins), thought of as "binary nodes" of a network, perform simultaneously to retrieve information, the latter being spread over the synapses, thought of as the (weighted) interconnections among nodes. However, common intuition of parallel processing is not only the "underlying" parallel work performed by the neurons to retrieve say an image -a book cover-, but instead, for instance, reading the manuscript, while keeping it securely in hand and noticing beyond its edges the room where we are reading in. A step forward standard parallel processing could be managing the main figure (the book) and a recognized background, and still maintaining available the capacity of further retrieve as a safety mechanism.

Standard Hopfield networks are not able to accomplish this kind of parallel process (apart from the network studied by Cugliandolo and Tsodsky [10], where multiple, not-spurious, patterns were contemporary recalled thanks to the correlations among them, the network studied by Coolen and Noest [8, 9], where partial inhibition of a single pattern recovery were allowed by chemical modulation or the approaches with integrate and fire neurons of Amit Bernacchia and Yakovlev [3], which are far away from the Hopfield framework). Indeed, spurious states cannot be looked at as the contemporary retrieval of several patterns, being rather unwanted outcomes, yielding to a glassy blackout [2]. Such a limit of Hopfield networks can be understood by focusing on the deep connection (in both direct [4] and inverse [14] approach) with restricted Boltzmann machines (RBM) [7]. Given a machine with its set of visible (neurons) and hidden (training data) units, one gets, under marginalization, that the thermodynamic evolution of the visible layer is equivalent to that of an Hopfield network. It follows that an underlying fully-connected bipartite restricted machine necessarily leads to bit strings of length equal to the system size and whose retrieval requires an orchestrated arrangement of the whole set of spins. This implies that no resources are left for further tasks, which is, from a biological point of view, too strong an oversimplification.

^{*}Università di Parma, Dipartimento di Fisica, Viale Usberti 7, 00198, Parma, Italy and INFN Gruppo collegato di Parma

[†]Sapienza Università di Roma, Dipartimento di Fisica, Piazzale Aldo Moro 2, 00185 Roma, Italy

[‡]Sapienza Università di Roma, Dipartimento di Fisica, Piazzale Aldo Moro 2, 00185 Roma, Italy and INFN Sezione di Roma

[§]Sapienza Università di Roma, Dipartimento di Fisica, Piazzale Aldo Moro 2, 00185 Roma, Italy

[¶]Sapienza Università di Roma, Dipartimento di Fisica, Piazzale Aldo Moro 2, 00185 Roma, Italy

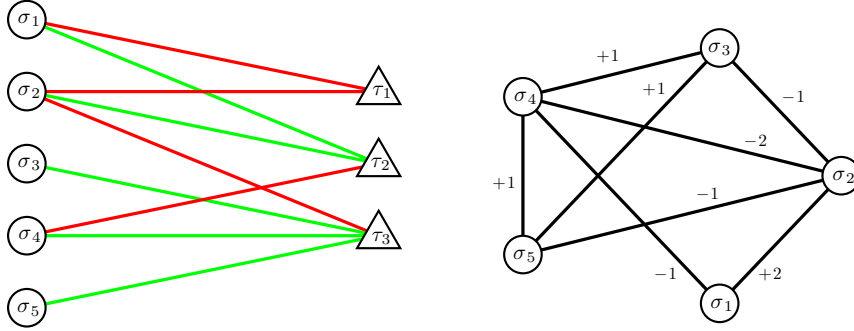


Figure 1: Schematic representation of a diluted restricted Boltzmann machine made up of $N = 5$ elements and $P = 3$ (left) and its corresponding weakened associative network (right). On the latter, the three patterns appear as $\xi^1 = [-1, -1, 0, 0, 0]$, $\xi^2 = [+1, +1, 0, -1, 0]$, $\xi^3 = [0, -1, +1, +1, +1]$ and the weight associated to each link (i, j) is $\sum_{\mu} \xi_i^{\mu} \xi_j^{\mu}$.

Here we introduce a possible way to relax this feature: Starting from a RBM we perform dilution on its links in such a way that nodes in the external layer are connected to only a fraction of nodes in the inner layer (see fig.1, left). As we show, this leads to a "weakened" associative network which, for non-extreme dilutions, is still embedded in a fully connected topology, but the bit-strings encoding for information are sparse (i.e. their entries are $+1, -1$ as well as 0) (fig.1, right).

More precisely, let us denote the P dichotomic spins making up the external layer as $\tau_{\mu} = \pm 1, \mu \in [1, \dots, P]$ and the N dichotomic spins making up the internal layer as $\sigma_i, i \in [1, \dots, N]$. RBMs admit an Hamiltonian description such that we can write

$$H(\sigma, \tau; \xi) = \frac{1}{\sqrt{N}} \sum_{i, \mu} \xi_i^{\mu} \sigma_i \tau_{\mu},$$

where we called ξ_i^{μ} the (quenched) interaction strength between the i^{th} spin of the inner layer with the μ^{th} spin of the external layer (possibly to be extracted from a proper probability distribution $P(\xi_i^{\mu})$). Usually one defines $\alpha = \lim_{N \rightarrow \infty} P/N$ as the storage value; in this first work we deal with the "low storage" regime, i.e. $P \sim \log N$, corresponding to $\alpha = 0$.

2 Statistical mechanics and signal to noise analysis

The thermodynamics of the system is then obtained by explicit calculation of the (quenched) free energy via the partition function, which read off respectively as

$$f(\alpha = 0, \beta) = \lim_{N \rightarrow \infty} \frac{1}{N} \mathbb{E} \log Z_{N, P}(\beta), \quad (1)$$

$$Z_{N, P}(\beta) = \sum_{\sigma, \tau} \exp \left(-\beta H(\sigma, \tau; \xi) \right). \quad (2)$$

A key point here is that the interaction is already one-body in each layer, such that marginalizing over one spin variable is straightforward and gives (expanding up to second order the hyperbolic sine)

$$\begin{aligned} Z_{N, P}(\beta) &= \sum_{\sigma} \prod_{\mu=1}^P \left[\cosh \left(\frac{\beta}{\sqrt{N}} \sum_i \xi_i^{\mu} \sigma_i \right) \right] \\ &= \sum_{\sigma} e^{\frac{\beta^2}{2N} \sum_{i, j} \sum_{\mu=1}^P \xi_i^{\mu} \xi_j^{\mu} \sigma_i \sigma_j} = \sum_{\sigma} e^{-N \sum_{\mu=1}^P m_{\mu}^2}, \end{aligned} \quad (3)$$

where we introduced the P Mattis magnetization $m_{\mu} = N^{-1} \sum_i \xi_i^{\mu} \sigma_i$. When $P(\xi_i^{\mu} = +1) = P(\xi_i^{\mu} = -1) = 1/2$ the Hamiltonian implicitly defined in eq. 3 recovers exactly the Hopfield model (at a rescaled

noise level β^2) and the ansatz of pure state, i.e. $\mathbf{m} = (1, 0, \dots, 0)$ (under permutational invariance), correctly yields the proper minimization of the free-energy in the low-noise limit. This means that, once equilibrium is reached, the state of the system σ will be parallel (under gauge invariance) to the pattern ξ^1 , phenomenon which is understood as recovery of a pattern of information.

As anticipated, here we remove the hypothesis of fully-connection for the bipartite network, diluting randomly its links in such a way that the coupling distribution gets

$$P(\xi_i^\mu) = (D/2)\delta_{\xi_i^\mu - 1} + (D/2)\delta_{\xi_i^\mu + 1} + (1 - D)\delta_{\xi_i^\mu},$$

where $D \in [0, 1]$ is a proper dilution parameter. It is easy to see that with this distribution, after marginalizing over one party as usual, we get an associative network, where the P patterns ξ^μ ($\mu = 1, \dots, P$) now contain zeros, on average for a fraction $(1 - D)$ of their length. As a result, the pure state ansatz can no longer work. In fact, now, the retrieval of a pattern does not employ all available spins and those corresponding to null entries can be used to recall other patterns: This is because the energy is a quadratic form in the Mattis magnetizations; its minimization requires that further patterns (up to the exhaustion of all available spins) are recalled in a hierarchical fashion. More precisely, the (thermodynamical and quenched) average of the Mattis magnetization of the k^{th} pattern retrieved is $D^k(1 - D)$, that is the overlap with the spins still available is maximized. The overall number of retrieved patterns K therefore corresponds to $\sum_{k=0}^K D(1 - D)^k = 1$, with the cut-off at finite N as $D(1 - D)^K \geq N^{-1}$ due to discreteness. For non pathological D (i.e. $D \neq 1, 0$ and not a function of N), this implies $K \lesssim \log N$, which can be thought of as a ‘‘parallel low-storage’’ regime of neural networks¹.

Before proceeding with the thermodynamic analysis, it is important to stress that the dilution introduced here is deeply different from the one introduced early by Sompolinsky [13] and more recently by Coolen [15], who showed how to solve the Hopfield model embedded in random networks, ranging from Erdős-Renyi graphs to small-worlds. In those systems, obtained by diluting directly the Hopfield network, the exciting results were the robustness of the retrieval under dilution: In particular, the Hopfield model was shown to be able to retrieve up to 80% of link removal, but still retaining a single pattern retrieval.

Figure 2 allows to appreciate how the behavior of the system is affected by the level where dilution is performed (either on the underlying bi-layer as we do or on the associative network directly): It represents, respectively, the distributions $P_{\text{pattern}}(\varphi_i)$ and $P_{\text{link}}(\varphi_i)$ of the signal insisting on spin i , namely $\varphi_i = \sum_{j=1}^N J_{ij}\sigma_j$, as a function of the related degree of dilution and calculated at zero noise level. Of course, when dilution is zero both distributions recovers the Hopfield model.

If we introduce a dilution à la Sompolinsky, since dilution affects directly links, only a fraction D of the N available spins participates to the field insisting on i so that the average value as well as the span of φ_i gets smaller as dilution is increased (Fig. 2, left). A very different scenario emerges when dilution is performed on patterns: As $D \neq 1$, $P_{\text{pattern}}(\varphi_i)$ gets broader and peaked at smaller values of fields. While the latter effect is trivial as the couplings are, on average, of smaller magnitude, the former effect deserves more attention. At β , N and P fixed, when dilution is introduced in bit-strings, couplings are made *uniformly* weaker (this effect is analogous to a rise in the fast noise) so that the distribution of spin configurations and, consequently also $P(\varphi; \beta, D, N, P)$, gets broader. At small values of dilution this effects dominates, while at larger values the overall reduction of coupling strengths prevails and fields get not only smaller but also more peaked (see Fig. 2, right). These different field distributions are expected to produce different physics; in particular our field is expected to allow parallel retrieval of patterns: To check robustness of these multiple basins of attractions, we perform a signal-to-noise analysis (at zero fast noise); for further simplicity we focus here only on $P = 2$ and, calling k_i a random variable uniformly distributed on $[-1, +1]$, we ask for stable states of the form $\sigma_i = \xi_i^1 + \delta(\xi_i^1)[\xi_i^2 + \delta(\xi_i^2)k_i]$, by which we can distinguish different possible configurations:

- $\forall i : \xi_i^1 \neq 0, \xi_i^2 = 0$ we get $\langle \text{signal} \rangle_\xi = D$, $\langle \text{noise} \rangle_\xi = 0$, $\langle (\text{noise})^2 \rangle_\xi = \alpha D^2$,
- $\forall i : \xi_i^1 \neq 0, \xi_i^2 \neq 0$ we get $\langle \text{signal} \rangle_\xi = (2D - D^2 \vee D^2)$, $\langle \text{noise} \rangle_\xi = 0$, $\langle (\text{noise})^2 \rangle_\xi = \alpha D^2$,
- $\forall i : \xi_i^1 = 0, \xi_i^2 \neq 0$ we get $\langle \text{signal} \rangle_\xi = D(D - 1)$, $\langle \text{noise} \rangle_\xi = 0$, $\langle (\text{noise})^2 \rangle_\xi = \alpha D^2$.

¹By taking D vanishing as a proper power of N , a ‘‘parallel high-storage’’ regime would also be possible, despite mathematically very challenging.

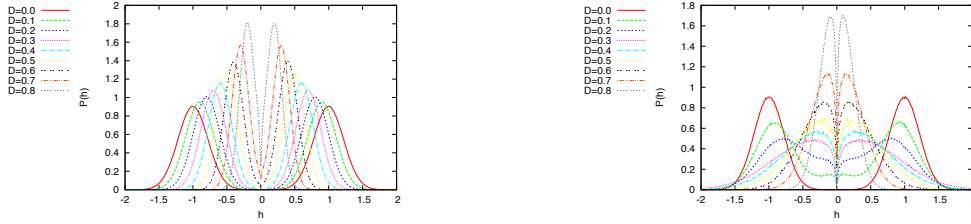


Figure 2: Distributions of the fields acting on the spins in the case of dilution a' la Sompolinsky (left) and of dilution directly in the bipartite network (right), shown for various percentages of dilution. In the former case D represents the average fraction of cut links, in the latter case D represents the average fraction of null pattern entries. Notice that as D is increased, at left, $P(h)$ behaves monotonically corresponding to an Hopfield model embedded on an Erdos-Renyi more and more sparse, while -at right- $P(h)$ does not behaves monotonically and the model is still defined on a fully connected topology.

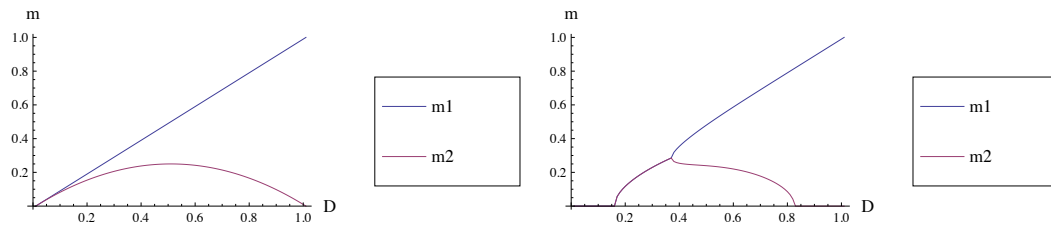


Figure 3: Two patterns analysis: (up) Analytical solution at $\beta = 10^4$. (down) Analytical solution at $\beta = 6.66$. All these curve have been checked versus Monte Carlo simulations (not shown) on Cuda processors with N up to 100000 spins with overall perfect agreement.

Hence, in the low-storage regime $\alpha = 0$ (and in the limit $\beta \rightarrow \infty$), we expect stable retrieved states of amplitude $m^1 = D$ and $m^2 = D(1 - D)$, in agreement with the scaling previously outlined.

To confirm this scenario we solve the statistical mechanics of the model. We stress that as no slow noise due to an extensive amount of patterns is at work ($\alpha = 0$), replica trick or techniques stemmed from disordered system theory [12, 6], are not necessary. We introduce a generic vector for Mattis magnetizations as $\mathbf{m} = (m_1, \dots, m_P)$, a density of the states $\mathcal{D}(\mathbf{m}) = 2^{-N} \sum_{\sigma} \delta(\mathbf{m} - \mathbf{m}(\sigma))$ and we write the free-energy density as

$$f(\beta) = \frac{\ln 2}{\beta} + \frac{1}{\beta N} \log \int d\mathbf{m} \mathcal{D}(\mathbf{m}) \exp\left(\frac{1}{2} \beta N \mathbf{m}^2\right). \quad (4)$$

After some algebra this equation becomes

$$f(\mathbf{m}, \mathbf{x}) = -\frac{1}{N} \int d\mathbf{m} d\mathbf{x} \exp\left(-N\beta \tilde{f}(\mathbf{m}, \mathbf{x})\right), \quad (5)$$

$$\tilde{f}(\mathbf{m}, \mathbf{x}) = -\frac{1}{2} \mathbf{m}^2 - i\mathbf{x} \cdot \mathbf{m} - \frac{1}{\beta} \langle \log 2 \cos[\beta \xi \cdot \mathbf{x}] \rangle_{\xi}, \quad (6)$$

which gives standard saddle point equations $\mathbf{m} = \langle \xi \tanh(\beta \xi \cdot \mathbf{m}) \rangle_{\xi}$, whose numerical solution for the case $P = 2$ is shown in Fig.3.

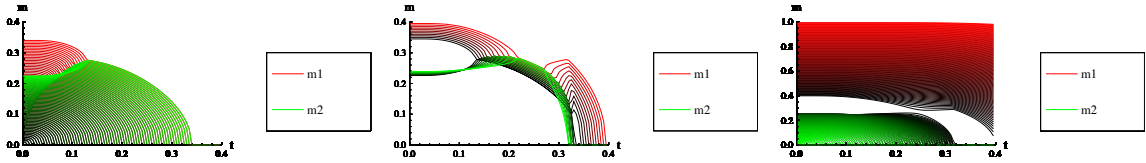


Figure 4: Two patterns phase diagram: (a) Analysis in temperature $t = \beta^{-1}$ for $D \in (0.00, 0.34)$. (b) Analysis in temperature $t = \beta^{-1}$ for $D \in (0.35, 0.40)$. (c) Analysis in temperature $t = \beta^{-1}$ for $D \in (0.41, 1.00)$.

3 Performances of the parallel processing network

For zero noise level, at it should, we have a perfect agreement with the signal to noise prediction and a confirmation of the parallel capabilities of the network: at a given value of D , say $D = 0.6$, two patterns are recalled together, perfectly recognized by the network.

In the presence of noise, network performances depends significantly on dilution: For small D , only the first pattern can be retrieved (because the fast noise is greater than the signal to channel two (i.e. m^2)) and the parallel ansatz reduces to the standard pure one (which can be seen as a particular case of the former). This Hopfield-like behavior persists as long as $D(1 - D) < \beta^{-1}$, above which m^2 also starts to grow and somehow recollects the related zero-noise curve. At intermediate degree of dilution the two magnetizations m^1, m^2 collapse and their amplitude decreases monotonically towards zero. When $D \sim 0$, the signal of any magnetization is smaller than the fast noise so that retrieval is no longer possible and the system behaves paramagnetically. We now explain in more details these features: We focus on the critical points corresponding to the vanishing of magnetizations and to the bifurcation points, by analyzing in details the simplest case of two patterns.

Solving the self consistency equations for two patterns we find

$$\begin{aligned} m_1 &= D(1 - D) \tanh(\beta m_1) + \frac{D^2}{2} [\tanh(\beta y) + \tanh(\beta x)], \\ m_2 &= D(1 - D) \tanh(\beta m_2) + \frac{D^2}{2} [\tanh(\beta y) - \tanh(\beta x)], \end{aligned}$$

where $x = m_1 - m_2$ and $y = m_1 + m_2$. The critical noise level at which the magnetizations disappear can be obtained by expanding the self-consistent equation for m_2 , namely $m_2 \sim D\beta m_2 + O(m_2^3)$. Form a standard fluctuation analysis [5, 11] therefore the critical noise level for the two patterns turns out as $\beta_c = \frac{1}{D}$, which of course reduces to $\beta_c = 1$ for the standard Hopfield model away from saturation [2].

We now expand for x small, such that the leading term is

$$x \sim \left[\frac{D(1 - D)\beta}{\cosh^2(\beta m_1)} + \beta D^2 \right] x + O(x^3), \quad (7)$$

by which, we obtain the critical value of β corresponding to the bifurcation is

$$\beta_c^{bif} = \left(D^2 \left[1 + \frac{D}{(1 - D)} \frac{1}{\cosh^2(\beta_c^{bif} m_1)} \right] \right)^{-1}. \quad (8)$$

Calculations leading critical behaviors can be easily extended to the case $P > 2$ and an extensive treatment of the network performances can be found elsewhere [1]. To understand bifurcations physically, we can divide spins into four classes ²:

- the set \mathcal{S}_1 contains spins i corresponding to zero entries in both patterns, namely $\xi_i^1 = \xi_i^2 = 0$; the cardinality of this set is $|\mathcal{S}_1| = (1 - D)^2$.
- the set \mathcal{S}_2 contains spins such that $|\xi_i^1| \neq |\xi_i^2|$; $|\mathcal{S}_2| = 2D(1 - D)$. Such spins tend to align with the related patterns being scarcely affected by the remaining ones.
- the set \mathcal{S}_3 contains spins corresponding to two parallel, non-null entries, that is $\xi_i^1 = \xi_i^2 \neq 0$; the number

²in general classes are $P + 1 + \sum_{k=0}^P \lfloor \frac{P-k}{2} \rfloor$

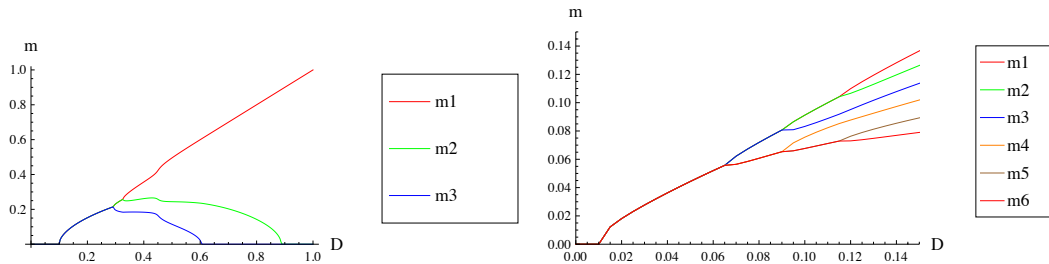


Figure 5: (left) Example of retrieval of three patterns. (right) Zoom on the behavior of multiple bifurcations with six recalled patterns. Note that similarities with the Ulam maps mirror the same similarities shared by the Hamiltonian.

of such spins is $|\mathcal{S}_3| = D^2/2$. These spins are the most stable.

- the set \mathcal{S}_4 includes spins i corresponding to two parallel, non-null entries, that is $\xi_i^1 = -\xi_i^2 \neq 0$, $|\mathcal{S}_4| = D^2/2$. These spins are intrinsically frustrated.

Therefore, we expect that the most prone spin to align with the related patterns are those in \mathcal{S}_3 , which can overall enjoy a field $\varphi_i = D^2$. The field gets effective when $D^2 > \beta^{-1}$.

Now, \mathcal{S}_2 is the next class to accomplish alignment and the field insisting on each spin is $\varphi_i = D^2 + D(1-D)$ so that when $D < \beta^{-1}$, the magnetization starts to grow. Up to now there is perfect symmetry between m_1 and m_2 and they grow paired. The growth proceeds paired until the magnetizations get the value $m_1 = m_2 = D^2/2 + D(1-D)$, where the former contribute comes from spins aligned with both patterns and the latter from single spins. At this point there is the saturation of \mathcal{S}_2 . From this dilution onwards one pattern must prevail over the other: m_1 grows and m_2 must necessarily decrease of the same amount.

The research of this paper belongs to the strategy funded by the FIRB grant RBFR08EKEV. Financial supports by Sapienza Università di Roma and INFN are acknowledged too. AB is grateful to Alberto Bernacchia and Ton Coolen for useful conversations.

References

- [1] E. Agliari, A. Barra, A. Galluzzi, F. Guerra, F. Moauro, *Parallel processing capabilities of immune networks*, to appear.
- [2] D.J. Amit, *Modeling Brain Function*, Cambridge University Press (1989).
- [3] D.J. Amit, A. Bernacchia, V. Yakovlev, *Multiple object working memory: A model for behavioral performance*, Cerebral Cortex **13**, 435-443, (2003).
- [4] A. Barra, A. Bernacchia, E. Santucci, P. Contucci, *On the equivalence of Hopfield Networks and Boltzmann Machines*, arXiv:1105.2790, (2011).
- [5] A. Barra, E. Agliari, *Equilibrium statistical mechanics on correlated random graphs*, J. Stat. Mech. 02027, (2011).
- [6] A. Barra, F. Guerra, G. Genovese, *The replica symmetric behavior of the analogical neural network*, J. Stat. Phys. **140**, 4, 784, (2010).
- [7] Y. Bengio, *Learning Deep Architectures for Artificial Intelligence*, Machine Learning **2**, 127, (2009).
- [8] A.C.C. Coolen, A.J. Noest, *Selective Pattern Recall in Neural Networks by Chemical Modulation*, J. Phys. A **23**, 575-579, (1990).

- [9] A.C.C. Coolen, A.J. Noest, G.B. de Vries, *Modelling Chemical Modulation of Neural Processes*, Network **4**, 101-116, (1993).
- [10] L.F. Cugliandolo, M.V. Tsodyks, *Capacity of networks with correlated attractors*, J. Phys. A **27**, 741, (1994).
- [11] F. Guerra, *Sum rules for the free energy in the mean field spin glass model*, Math. Phys. in Math. and Phys., F.I.C. **30**, 161-170, (2001).
- [12] M. Mézard, G. Parisi and M. A. Virasoro, *Spin glass theory and beyond*, World Scientific, Singapore (1987).
- [13] H. Sompolinsky, *Neural networks with non-linear synapses and a static noise*, Phys. Rev. A **34**, 2571-2584, (1986).
- [14] G. Tkacik, E. Schneidman, M. J. Berry II, W. Bialek, *Spin glass models for a network of real neurons*, arXiv.org, q-bio, arXiv:0912.5409, (2009).
- [15] B. Wemmenhove, A.C.C. Coolen, *Finite Connectivity Attractor Neural Networks*, J. Phys. A **36**, 9617-9633, (2003).